Accident Analysis and Prevention 66 (2014) 43–54

Contents lists available at ScienceDirect

Accident Analysis and Prevention

journal homepage: www.elsevier.com/locate/aap

High strength steels, stiffness of vehicle front-end structure, and risk of injury to rear seat occupants

Elham Sahraei[a,*], Kennerly Digges[b], Dhafer Marzougui[c], Kim Roddis[b]

[a] Massachusetts Institute of Technology, 77 Mass Ave, room 5-218B, Cambridge, MA 02139, USA
[b] The George Washington University, Washington, DC, USA
[c] The George Mason University, Fairfax, VA, USA

ARTICLE INFO

Article history:
Received 11 April 2013
Received in revised form
18 November 2013
Accepted 4 January 2014

Keywords:
Vehicle stiffness
Risk of injury
Rear sear occupant
Finite element model

ABSTRACT

Previous research has shown that rear seat occupant protection has decreased over model years, and front-end stiffness is a possible factor causing this trend. In this research, the effects of a change in stiffness on protection of rear seat occupants in frontal crashes were investigated. The stiffness was adjusted by using higher strength steels (DP and TRIP), or thicker metal sheets. Finite element simulations were performed, using an LS Dyna vehicle model coupled with a MADYMO dummy. Simulation results showed that an increase in stiffness, to the extent it happened in recent model years, can increase the risk of AIS3+ head injuries from 4.8% in the original model (with a stiffness of 1000 N/mm) to 24.2% in a modified model (with a stiffness of 2356 N/mm). The simulations also showed an increased risk of chest injury from 9.1% in the original model to 11.8% in the modified model. Distribution of injuries from real world accident data confirms the findings of the simulations.

1. Introduction

Use of high strength steels in vehicle structures has potential in weight reduction and improving certain safety features. As a result, the vehicle stiffness in all directions may increase. A higher stiffness of the vehicle structure can have safety benefits to occupants by decreasing the intrusion to the occupant compartment. However, it can also affect the crash pulse of the vehicle and the accelerations transmitted to the occupants. Front seat occupants are protected against such elevated crash pulses by advanced airbags and force limiting, pretentioning seatbelts. Safety features for rear seat occupants, however, have not changed by any measurable means since introduction of three-point belts in the rear seat. Therefore, the net effects of an elevated crash pulse on protection of rear-seat occupants needs to be fully understood.

Earlier studies showed that rear seat occupants were protected better than front seat occupants in the older model years of vehicles (Berg et al., 2000; Evans and Frick, 1988; Kuppa et al., 2005; Sahraei et al., 2009; Smith and Cummings, 2004). Perception of safety in the rear seat might even weaken incentives for use of seatbelts by rear seat occupants, as only 60% of rear seat occupants in tow-away crashes were reported to be belted (Parenteau and Viano, 2003). However, the protection of rear seat occupants has decreased in recent model years (Sahraei et al., 2009, 2010; Sahraei and Digges, 2009). Consequently, adult occupants seem to be less protected in rear seats compared to the right front seat (Bilston et al., 2010; Sahraei et al., 2010; Smith and Cummings, 2006). The relative reduction in protection of rear seat occupants compared to front seat occupants is often explained to be a result of emergence of advanced safety features and improved protection for the front seat occupants (Beck et al., 2009; Kent et al., 2007). However, the absolute increase in risk of injury to rear seat occupants (Sahraei and Digges, 2009) could not be a function of advanced airbags or force-limiting belts in the front seat.

It is reported that front-end stiffness of vehicles have increased over model years (Sahraei et al., 2011; Swanson et al., 2003) and such an increase in stiffness could be the cause of a decrease in protection of rear seat occupants (Sahraei et al., 2013). In the present study, finite element modeling was used to isolate the effect of an increase in stiffness from other changes in platform and safety features of vehicles, and to quantify the changes in risk of injury to rear seat occupants due to change in stiffness. In an earlier publication from this research, it was shown that scaling the strength of steel, changing the mass of the vehicle, or thickness of load bearing structure can change stiffness and affect head and chest accelerations (Sahraei et al., 2011). In this paper, a more thorough validation of the model was performed to make sure the model can predict risk of injury to head, chest, and neck of the occupant. In addition to revisiting the effect of change in stiffness by former methods, change of stiffness due to using DP and TRIP steels in the front

* Corresponding author. Tel.: +1 617 324 5025.
E-mail address: elhams@mit.edu (E. Sahraei).

0001-4575/$ – see front matter © 2014 Elsevier Ltd. All rights reserved.
http://dx.doi.org/10.1016/j.aap.2014.01.004

structure was studied. Also, the effects of a change in stiffness in a lower speed crash, and an angle impact were evaluated. Another factor that was considered to affect protection of rear seat occupant and was studied in this research was the space available for the rear seat occupant and relative distance to the back of the front seat.

2. Finite element models of vehicle, dummy and the seatbelt

National Crash Analysis Center has a library of finite element models of vehicles developed in LS-Dyna for crashworthiness studies (NCAC, 2008). The Ford Taurus FE model is one of the most detailed models of a medium size passenger car in that library. This vehicle model was validated at NCAC against NHTSA full frontal crash test 3248. The available model was improved by adding a seat cushion in the rear seat and, also, by increasing the floor thickness by 0.2 mm to account for mats and floorings not included in the original model.

The model was to be used for evaluating the protection of rear seat occupants. Therefore, an actual crash test performed using a Ford Taurus at National Highway Traffic administration which had dummies in the rear seat was used to validate the model (Test 5143). The initial speed of the vehicle was set to 56 km/h. The test set-up was according to New Car Assessment Program (NCAP) settings. The actual crash test had two 5 percentile female Hybrid III dummies in the front seats, however, as those dummies were not to be used for this study, only their mass (50 kg each) was added to the vehicle front seats. Locations of accelerometers were adjusted to be exactly similar to NHTSA crash test 5143. The FE vehicle model had 972,148 elements and 921,937 nodes. Out of this total, 837,673 were shell elements (705 shell parts), 134,459 solid elements (82 solid parts), 4 beam elements (2 beam parts), 12 discrete elements (5 discrete parts), and 124 mass elements.

The rear seat dummy in the NHTSA test was a 5 percentile female Hybrid III dummy. In the simulations, the rear seat dummy was modeled using MADYMO multi-body dynamics software. MADYMO dummies are validated against component tests as well as sled type simulations. After an initial evaluation of both the facet model and the ellipsoid model, the results showed that the ellipsoid model was not as reliable as the facet model for our purpose. Therefore, the facet dummy was used for this study.

The dummy model was coupled with the vehicle model using LS Dyna-MADYMO coupling tools. A settling simulation was performed to make sure the dummy was positioned correctly on the seat cushion and the seat cushion was deformed to the contour of the dummy. The deformed shape of the seat and the residual stresses in the foam elements of the seat were then extracted from this simulation and input into the vehicle model. Dummy joint positions after settling were also extracted and imported into the dummy model to reflect the correct positioning of upper and lower limbs relative to the seat. The FE mesh for the three-point belt was developed using MADYMO and Hypermesh. The D-ring and retractor were added using LS Dyna seatbelt elements. The fabric model was based on properties of the Automotive Occupant Restrains Council (AORC) received from Livermore Software Technology Corporation (LSTC), and the lock acceleration was 0.7*g* according to Federal Motor Vehicle Safety Standard (FMVSS) 209.

Our previous coupled vehicle–dummy–belt models were validated for head and chest acceleration, but the dummy chest deflection was not validated. In this study, as the risk of AIS3+ injury had to be calculated, there was a need to have proper representation of the chest deflection. A proper contact between the LS Dyna belt and the MADYMO dummy chest and neck is essential to model

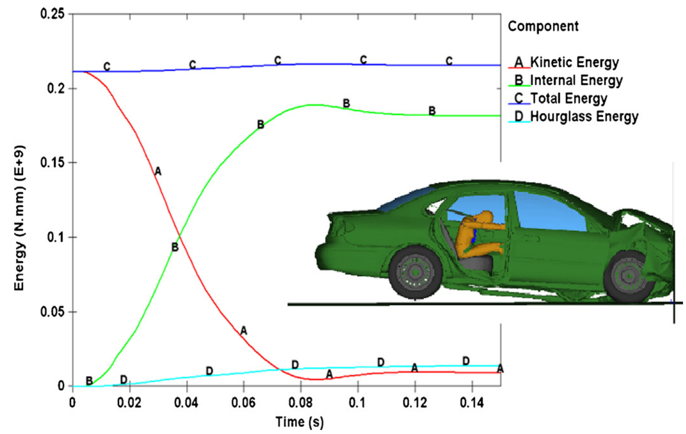

Fig. 1. Balance of energies through the finite element simulation.

chest deflection correctly. None of the MADYMO contacts alone simulated the chest, neck, and belt interactions correctly. The node to surface contact allowed for some penetration of the belt into the chest, and the surface to surface contact resulted in slipping of the belt over the thorax. However, the use of two contacts (node to surface + surface to surface) at the same time solved this problem. Proper simulation of the belt/dummy interactions affected accelerations of head and chest of the dummy, as well. Therefore, a full validation was required to make sure that the updated model represents the actual crash test.

2.1. Validation of the model

A Ford Taurus NCAP test was used for comparison with the simulated Ford Taurus vehicle. The two models were similar in terms of model year (2004 versus 2001), mass (1739 kg versus 1740 kg), length (5025 mm versus 5022 mm), width (1865 mm versus 1853 mm), and location of the center of gravity from front axle (1156 mm versus 1070 mm).

At the first step the model balance of kinetic, internal, hourglass and total energies was reviewed, see Fig. 1. The kinetic energy drops as the vehicle hits the rigid wall, and the internal energy increases as the deformation progresses. The hourglass energy is less than 10% of the total energy through the simulation, and the total energy remains almost constant.

To quantify the validation of the simulation against the test, a method suggested by Ray (1996) was used. Ray studied the repeatability of crash tests and provided criteria for validating simulation results. He reported that repeating crash tests of exactly similar vehicles in standard conditions using the same equipment and procedures can still produce some variability in the measured accelerations. The differences in crash pulse of two identical tests can be associated with the variations in vehicle characteristics caused by different construction materials or imprecise construction methods. Small variations in impact condition and experimental errors in data collection also contribute to variations in crash pulse. Ray demonstrates that even two independent measurements of one crash test can show differences between time history results. He also provides a quantifiable criterion to judge the similarity of a crash test with a simulation above and beyond subjective comparison. In this method, the difference between the simulated acceleration and the test acceleration is calculated in each instant of the time, and it is assumed that these residuals are results of random experimental errors. The criteria suggest that the average of these residuals should be less than 5% and the standard deviation less than 20% of the peak acceleration. If these conditions are met, the simulation is considered the same event as the crash

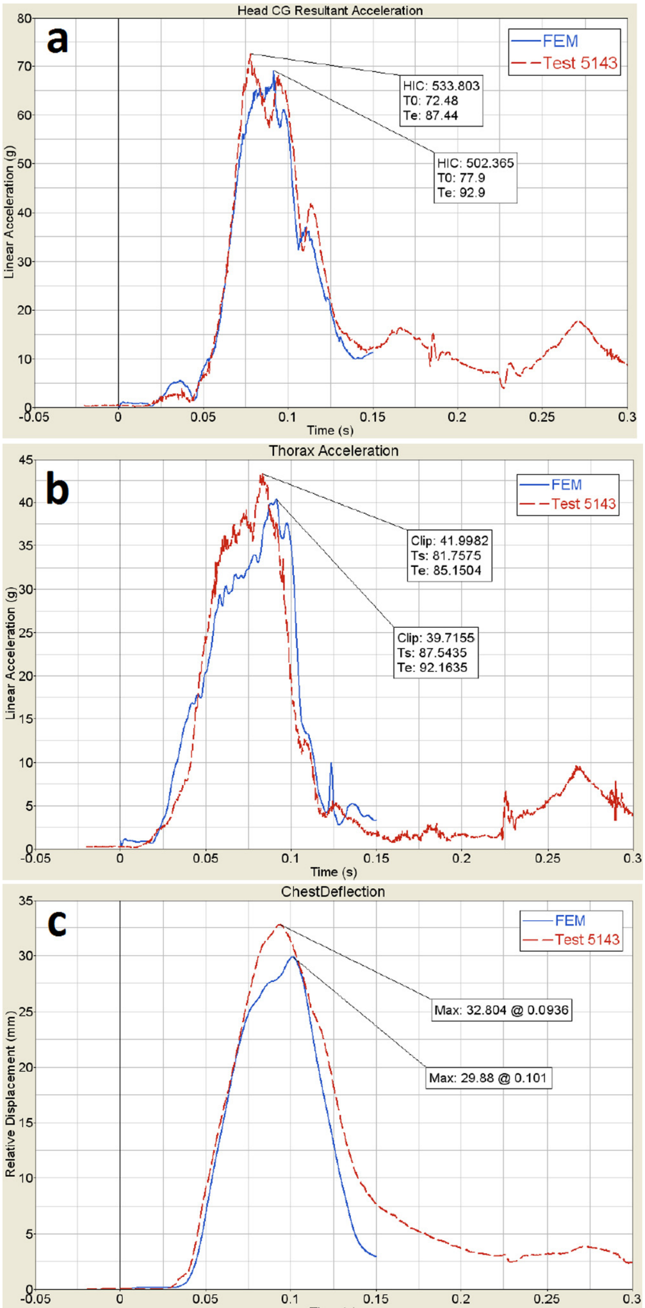

Fig. 2. Hybrid III 5 percentile dummy head acceleration (a), chest acceleration (b), and chest deflection (c) from simulation versus the ones from NCAP test.

test. RSVVP software developed for this purpose (Mongiardini and Ray, 2009) was used to calculate the residuals, their average and the standard deviation for each of the acceleration pulses of the vehicle and the dummy, see Appendix A. The normalized average of the X-acceleration of the top engine accelerometer was −0.02, and the normalized standard deviation was 0.15. For the left rear seat accelerometer, the normalized average was −0.01, and the normalized standard deviation was 0.14. All of these values meet the proposed criteria. Therefore, the vehicle model is validated for the representation of a real crash test.

Fig. 2a shows the resultant head acceleration of the dummy at the center of gravity. Using RSVVP software, the normalized average of residuals was calculated as −0.02, and the normalized standard deviation was 0.05. Both meet the proposed criteria for validation.

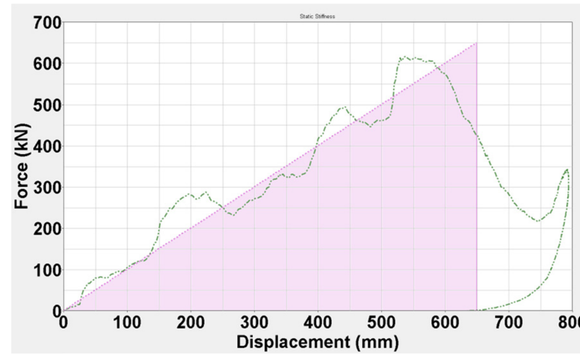

Fig. 3. Force–displacement curve of the simulated vehicle, and the estimated energy absorption from static stiffness (shaded area).

Fig. 2b shows the thorax acceleration of the test dummy versus the simulated dummy. The normalized average of the residuals for this comparison was 0.01, and the normalized standard deviation was 0.11. These values also pass the proposed criteria for validation. Fig. 2c shows the chest deflection of the dummy from simulation versus the crash test. The deflection curve is a displacement curve and cannot be validated using the proposed criteria; however, considering the visual similarity of the curves, it is considered valid for the purpose of this study.

2.2. Stiffness variations

The static stiffness, K, of the vehicle was calculated according to Swanson et al. (2003) from the following equation:

$$\frac{1}{2}mv^2 = \frac{1}{2}Kx^2$$

where m is mass, v is the initial velocity, and x is the total change in length of the vehicle. In this method of stiffness calculation, it is assumed that the initial kinetic energy transfers to an internal energy under a linear force–displacement trajectory up to final deformation of the vehicle. The rebounded portion of deformation is ignored in the calculation of energy. The static stiffness calculated by this method is close to the initial stiffness, or slope of the force–displacement curve, see Fig. 3. For the Ford Taurus model used in this study, the static stiffness was 1000 N/mm.

Eight values of static stiffness were generated in the model through following structural changes in the original model:

- In two models, the mass of the vehicle was increased by 10% and 20% (referred to M10 and M20 in the rest of the text). The static stiffness for these two models was 912 N/mm and 902 N/mm, respectively.
- In two models, the strength (stress–strain curve) of the frontal load bearing structures was scaled up by 40% and 80% (Models S40 and S80), increasing the static stiffness to 1226 N/mm and 1557 N/mm.
- In one simulation, the load bearing rails of Model S40 were replaced with high strength Dual Phase steels DP 600 and DP 800 (Oliver et al., 2007), keeping the original ratio of strength between different members (Model S40DP) unchanged. The static stiffness for this model was 1377 N/mm.
- In one simulation, the load bearing rails of Model S40 were replaced with high strength Transformation Induced Plasticity steels of TRIP600 and TRIP800 (Oliver et al., 2007), keeping the original ratio of strength between different members (Model S40Trip) unchanged. The static stiffness for this model was 1328 N/mm.

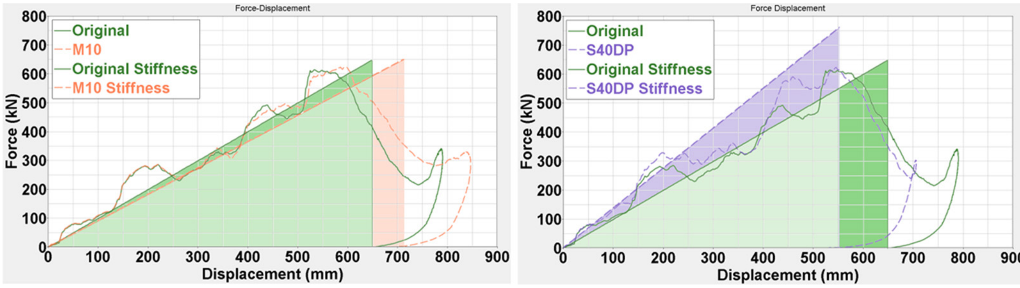

Fig. 4. Change in static stiffness due to increase in mass (left), or increase in strength of material (right).

- In one simulation, the thickness of frontal load bearing members was increased by 80% (Model T80). This model had the highest static stiffness of 2356 N/mm.

The range of produced static stiffness values in this study represents the change in average stiffness of vehicles in 1982–2010 model years of vehicles tested by NHTSA, where the average stiffness changed from 833 N/mm to 2037 N/mm in model years 1982 to 2010, respectively (Sahraei et al., 2011). Fig. 10 shows the force–displacement curve for the original model compared to M10 and S40DP models. The linear estimates of the curves through static stiffness calculations are shown with shaded triangles. The first noticeable change in the force–displacement curves of the models was the change in total deformation of the vehicle. With an increase in mass, the total deformation increases; and consequently, the estimated static stiffness decreases, see Fig. 4 left. In contrast, the increase in the strength of members decreases the total deformation and causes an increase in static stiffness, see Fig. 4 right.

All the models were simulated at 56 km/h frontal NCAP scenarios. Additionally, the original model and the model with highest stiffness (T80) were simulated in two lower speed frontal crash scenarios at 40 km/h (25 mph), with a full frontal rigid barrier contact and a 30 degree rotated rigid wall. This was done to make sure the effects studied in the NCAP simulation were not limited to full frontal high speed crashes and an increase in stiffness would cause similar trends of rear seat occupant protection in lower speeds and in angled crashes.

To put the effects of an increase in stiffness in perspective, another factor with probable effects on the protection of rear seat occupant was also investigated. That factor was the position of front seat relative to the rear seat occupant. In this final simulation, the right front seat of the vehicle (which was in the most forward position during previous simulations) was moved to the most rearward position possible for this car (Model RF seatback). To replicate the size of smaller passenger cars, the effects of a reduction in space for rear seat occupants were studied in this simulation.

For each simulation, head injury criteria (HIC), thoracic criteria (chest acceleration and chest deflection), and neck injury criteria (N_{ij}) were evaluated. HIC is a function of head acceleration integrated in a time domain to determine the possibility of head injuries in a given impact:

$$\mathrm{HIC} = \left\{ \left[\frac{1}{t_2 - t_1} \int_{t_1}^{t_2} a(t)dt \right]^{2.5} (t_2 - t_1) \right\}_{\max}$$

The maximum time domain $(t_2 - t_1)$ in the final rule regulation is 15 ms, which gives HIC15. The acceptable HIC15 value for Hybrid III adult dummies is 700 (Eppinger et al., 2000). Chest accelerations are measured in terms of g, and the injury limit for a 5 percentile female dummy is 60g. Chest deflection is the deformation of the chest measured in millimeters (mm), and the limit for a small female dummy is 52 mm. The acceptable value of neck injury criteria (N_{ij}) is one (Eppinger et al., 2000).

3. Results of NCAP simulations

Fig. 5 shows a comparison of three crash pulses from three model years of Ford Taurus vehicles tested by NHTSA versus three of the pulses generated in the above mentioned simulations. The NCAP test crash pulses shown in Fig. 5 are chosen to show the differences in crash pulse data of Ford Taurus vehicles in a three-decade span, i.e. test numbers 1385 (model year 1990), 3248 (model year 2000), and 6808 (model year 2010). The simulation crash pulses are from the original model, the model with a 40% increase in stiffness, and the model with an 80% increase in the thickness of load bearing frontal parts. It can be observed that with an increase in the model year of the vehicle, in NCAP tests, the peak deceleration increases and shifts forward in time. In the 1990 model year, the peak deceleration was −29g and occurred at 0.067 s, while in the 2010 model year, the peak deceleration was −46g and occurred at 0.049 s. Similar trends of increase in peak deceleration and forward shift in time were observed in simulations. The original model had

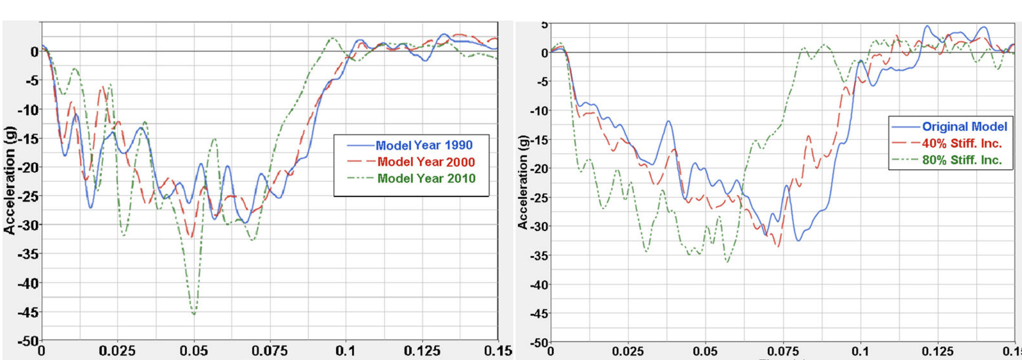

Fig. 5. Crash pulses from three generations of Ford Taurus NCAP tests (left) and crash pulses created in three of the simulations (right).

its peak deceleration at −32*g* and time 0.079 s. In the model with 80% thickness increase of load bearing frontal parts the peak in crash pulse was −36*g* at 0.056 s. It should be noted that the crash pulses in simulations were not expected to have perfect similarity with NCAP tests. The base model was validated against a relevant real crash test using an accepted quantifiable criterion in crashworthiness literature, as reported in Section 3.1. However, the changes of mass or stiffness in simulations are by no means the only changes in the structure of the tested vehicles through two decades. Designs of the body in whites of the vehicles have slight changes from one model year to the other. Construction equipment and materials also change through the years. Placement of data acquisition sensors in actual crash tests can have slight variations as well. Real world accidents and crash tests have shown a reduction in the protection of rear seat occupants and an increase in mass and stiffness of vehicles over model years. They also show a correlation between the increase in stiffness and the increase in injury predictions of dummies in the rear seats (Sahraei et al., 2009, 2010, 2013). In the simulations, we intend to isolate the effects of changes in mass and stiffness while keeping all other factors constant. This is to make sure the correlations observed in the real world are not due to another unaccounted-for cause, which is substituted by stiffness and model years of vehicles in the above statistical analyses. Such data does not exist in the real world because of all the above-mentioned changing variables through model years. Therefore, the crash pulses of a series of simulations performed in this study are not expected to represent the crash pulses of vehicles for any specific model year, and they differ with real crash tests in terms of pulse duration, pulse shape, and peak accelerations. They are presented and compared with NCAP tests only to point out the increase in peak acceleration and the shift in time.

Fig. 6a shows the increase in resultant head acceleration. The increase in head accelerations seem to be a direct consequence of increase in crash pulse, as there was not any contact observed between the head and vehicle parts. It can be observed that the head acceleration curve shifts backward and the peak increases with the increase in static stiffness. The HIC value also increases, accordingly. It should be noted that the increase in accelerations was not due to chin to chest contacts, which exist in some simulations. Timing of such contacts was much later than the time of peak acceleration. Also, a significant reduction of the peak acceleration was already observed before any chin to chest contact happened, and a second peak value in head acceleration due to such a contact was less than half of the first peak value. Furthermore, the time domains of chin to chest contacts, when existed, were far from the domain of HIC calculations. Fig. 6b and c shows similar trends for the chest acceleration and deflection curves. The 3 ms clip chest acceleration also increases with the increase in stiffness.

Table 1 gives the head, chest, and neck injury criteria values for all the simulations. HIC 15 for these simulations changes from 428 in the reduced mass model to 1027 for the model with the highest stiffness. In real NCAP tests with 5 percentile female dummies in the rear seats (Sahraei et al., 2013), the HIC15s were from 226 to 1160. Therefore, observed values in the simulations are within the range realized at real NCAP tests. It should be noted that the crash tests used in Sahraei et al. (2013) were all performed on vehicles of model years 2004–2005. There are no data publicly available on crash tests of other model year vehicles with dummies in the rear seats to verify changes of HIC with model year. However, their study proved a correlation between stiffness of vehicles and injury measures of dummies in the rear seats, using multiple regressions and considering vehicle speed during the test. They also showed an increase in the stiffness of vehicles with an increase in their model year using the database of all NCAP tests (please note that rear seat dummies are not present in all NCAP tests to allow for direct conclusion).

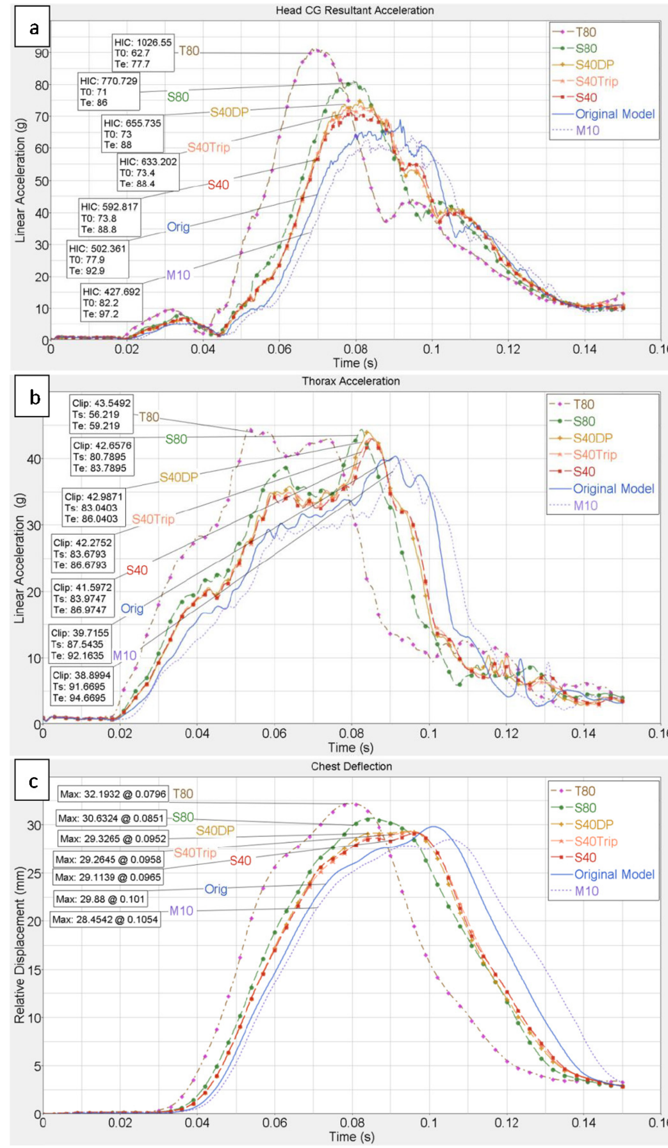

Fig. 6. Resultant head accelerations and HICs (a), thorax accelerations and 3 ms chest clips (b), and chest deflections and its maximum values (c) for simulations at 56 km/h frontal NCAP scenarios. In the legend, the original model represents the base model which was validated against a relevant crash test. In M10, the mass of the vehicle was increased by 10%. In Models S40 and S80, the strength of the frontal load bearing structures was scaled up by 40% and 80%. In S40DP, the load bearing rails of S40 were replaced with DP steels. In S40Trip, materials of same parts were replaced with TRIP steels.

The change of 3 ms clip chest acceleration for the simulations was from 39 gs to 43 gs within the range of 36–53 gs observed in real NCAP tests. The maximum chest deflection varied from 28 mm to 32 mm, again within 17–49 mm reported for NCAP tests.

Overall, the head, chest, and neck injury measures of the dummy in the rear seat seem to be sensitive to changes in the front end stiffness of the vehicle. Whether this increase in stiffness is due to an increase in the strength of the material, or the use of a thicker sheet of metal does not seem to cause a difference in the outcome.

To quantify the observed trends, linear regression models were fitted to the data. All four models associating stiffness to HIC15, 3 ms clip chest acceleration, chest deflection and were significant (as shown in Fig. 7). However, the N_{ij} regression model seems to be dominated by the last point of stiffness, and without that point no clear trend is observed.

Table 1
Vehicle crush and static stiffness and dummy's head, neck and chest injury criteria.

		Mass (kg)	Static stiffness (N/mm)	HIC 15	3 ms Clip chest acc (g)	Chest deflection (mm)	N_{ij}
Orig.	Original model	1740	1000	502	39.7	29.88	0.68
M10	Mass of vehicle increased by 10%	1910	912	427	38.8	28.45	0.67
M20	Mass increased by 20%	2080	902	475	37.2	27.27	0.73
S40	Stiffness of frontal rails increased by 40%	1740	1226	593	41.6	29.11	0.67
S40Trip	Modified parts of S40 model replaced with Trip steel	1740	1328	633	42	29.26	0.67
S40DP	Modified parts of S40 model replaced with DP steel	1740	1377	656	42.9	29.33	0.67
S80	Stiffness of frontal rails increased by 80%	1740	1557	771	42.8	30.63	0.71
T80	Thickness of frontal rails increased by 80%	1817	2356	1026	43.5	32.19	0.89

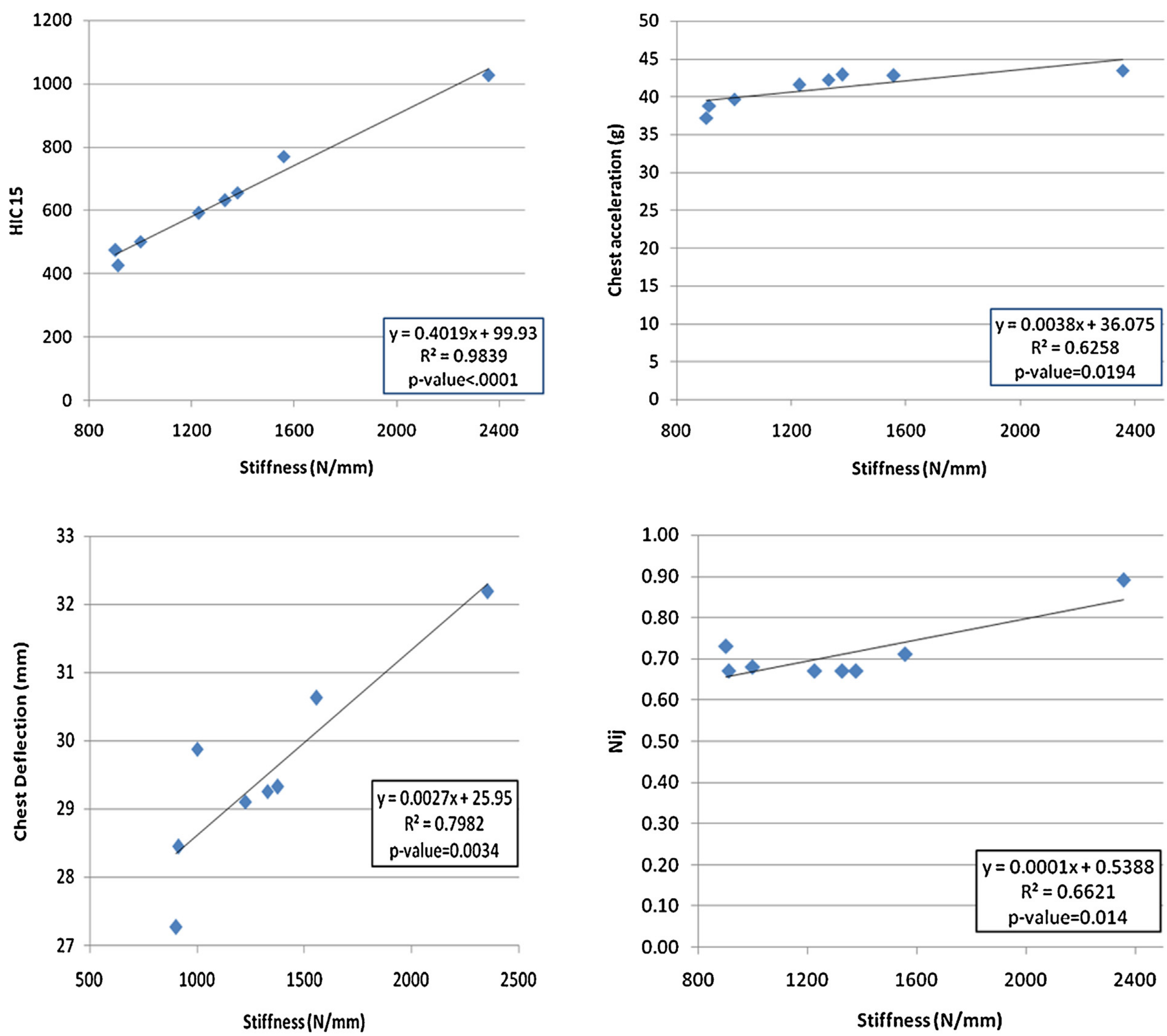

Fig. 7. Increase in HIC15, 3 ms clip chest acceleration, chest deflection, and N_{ij} with increase in static stiffness.

3.1. Risk of AIS3+ injury

Abbreviated injury scale (AIS) is a code to describe severity of a specific injury on a scale of 1 to 6. AIS1 denotes a minor and AIS6 describes an untreatable injury. In automotive crashworthiness applications, risk of AIS2 (moderate injury) or AIS3 (serious injury) is often used to characterize safety of different crash scenarios and protective countermeasures. In this context, the + sign after the AIS value means injuries with at least the denoted injury. For example, AIS3+ means injuries with AIS3 or more. In this section, the injury measures estimated through finite element modeling were used to estimate the risk of AIS3+ injury of head, chest, and neck for each step of changes in the structure of the vehicle. Several risk curves have been developed to estimate the risk of head injury based on HIC values (Hertz, 1993; Laituri et al., 2003; Mertz et al., 1996, 1997, 2003; Prasad and Mertz, 1985). For this research, the risk curves adopted by NHTSA were used to estimate the risks of AIS3+ injury based on dummy readings for the 5% female dummy (NHTSA, 2008). These curves estimate the risks for an occupant of average driving age (35 years old). Laituri et al. (2005) have developed a risk curve to estimate the risk of chest injury for different age groups of occupants. As several studies suggest a difference

Table 2
Injury risk curves used to estimate risks of AIS3+ injuries.

Injury Criteria	Risk curve
Head (HIC15)	$P_{head}(\text{AIS3+}) = \Phi\left(\ln(\text{HIC15}) - 7.45231/0.73998\right)$ where Φ = cumulative normal distribution
Chest Deflection (mm) (5% Female dummy) For 35 years old occupant	$P_{\text{chest-defl}}(\text{AIS3+}) = 1/(1 + \exp(10.5456 - 1.7212 \times (\text{ChestDefl})^{0.4612}))$
Chest Deflection (mm) Age dependent (years)	$P_{\text{chest-defl}}(\text{AIS3+}) = 1/(1 + \exp(12.597 - 0.05861Age - 1.7212 \times (\text{ChestDefl})^{0.4612}))$
Neck (N_{ij})	$P_{neck\_N_{ij}}(\text{AIS3+}) = 1/(1 + \exp(3.2269 - 1.9688N_{ij}))$

between rear seat protection of older (59+ years old) occupants and the younger ones (Kuppa et al., 2005; Sahraei et al., 2010), Laituri curve was used to estimate the risk of chest injury for 60 year old adults in each of the crash scenarios. All the risk curves used for this study are summarized in Table 2.

Table 3 shows the probability of AIS3+ injury for the head, chest, and neck based on the discussed risk curves. It can be observed that for the original model, the risk of AIS3+ head injury is about 5%. This risk increases with the increase in front end stiffness up to 24%. The risk of chest injury for a 35 years old occupant in the original model was about 9%. This risk increased to about 12% for T80 model. Risk of chest injury for a 60 years old occupant was about 30% in the original vehicle, and this risk increased to 37% for the T80 vehicle. Risk of neck injury was about 13% in the original model, and it increased up to a maximum of around 19% in the modified vehicle models. It should be noted that the risk estimates for neck injury according to NHTSA are expected to overestimate the risk of injury in real world crashes. An alternative method suggested by Prasad et al. (2010) reduced the estimate of risks of neck injury for all simulations to less than 1%.

3.2. Low speed frontal and oblique crash simulations

Two sets of simulations were performed at speeds of 40 km/h with a full frontal rigid barrier and a 30 degree angled rigid barrier. This was done to verify that similar trends observed in an NCAP full frontal crash test can be experienced during lower speed crashes and oblique crashes. Therefore, for each scenario, the simulation was repeated for the original model and the model with maximum stiffness, T80. Fig. 8 shows the head and chest accelerations as well as chest deflection of the 5% female dummy in the rear seat for the original model and the T80 model at a 40 km/h full frontal impact. It can be observed that all three curves have considerably increased for the T80 model when compared to the baseline model. This observation confirms that increasing stiffness causes an increase in risk of injury even in lower speed impacts, and that the results of the in depth NCAP study presented in the previous section is not limited to higher speed impacts.

For the models in the 30 degree oblique impact scenario, the barrier does not fully stop the vehicle, but redirects it during the impact. As the vehicle is not fully stopped, the injury measures for this impact are overall lower than those for the full frontal impact. Fig. 9 shows the head acceleration, chest acceleration, and chest deflection of the rear seat dummies in the original vehicle model and the T80 vehicle model in the oblique impact. Again, it can be observed that the dummy in the T80 model had higher head and chest accelerations as well as chest deflection when compared to the original model. Therefore, the association of front end stiffness and the risk of injury to rear seat occupants as fully discussed for NCAP tests is not limited to full frontal crashes, as similar trend was observed for the oblique impact as well.

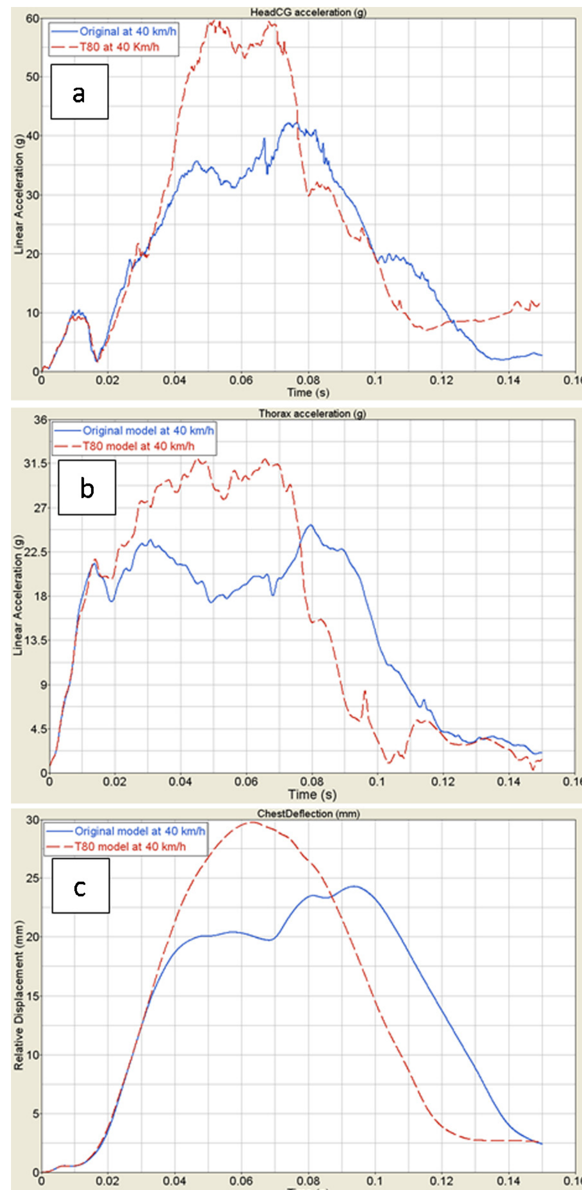

Fig. 8. Head acceleration (a), chest acceleration (b), and chest deflection for the original (solid line) and T80 (dash line) models at 40 km/h speed.

3.3. Moving right front seat to the most backward position

In the last simulation, the right front seat was moved to the most backward position. The dummy head did not contact back of the front seat even in this simulation. However, the backward

Table 3
Risk of AIS3+ injury based on injury reading of the 5% female dummy for 35 years old and 60 years old occupants.

	P_{Head}(AIS3+)%	P_{Chest}(AIS3+) (%) (35YO)	P_{Chest}(AIS3+) (%) (60YO)	P_{Neck}(AIS3+) (%) (NHTSA)	P_{Neck}(AIS3+) (%) (Prasad et al., 2010)
Original model	4.8	9.1	30.3	13.1	0.1
M10	3.0	7.7	26.5	12.9	0.1
M20	4.1	6.7	23.6	14.3	0.1
S40	7.5	8.3	28.2	12.9	0.1
S40DP	9.6	8.6	28.8	12.9	0.1
S40Trip	8.8	8.5	28.6	12.9	0.1
S80	13.8	9.9	32.3	13.8	0.1
T80	24.2	11.8	36.7	18.6	0.5

movement of the seat caused a severe contact between dummy's left hand and the front seat back. Considering the high frequency of upper extremities in distribution of AIS2+ injuries, and also high frequency of front seat back as source of injury (Sahraei and Digges, 2009), this simulation can clarify role of front seat back in causing upper extremity injuries.

Fig. 10 shows the head acceleration, chest acceleration, and chest deflection of the dummy from the original model versus the model with the right front seat moved to the most backward position. A slight increase in head and thorax acceleration and a slight decrease in chest deflection can be observed from these figures. The reduction in chest deflection could be due to an

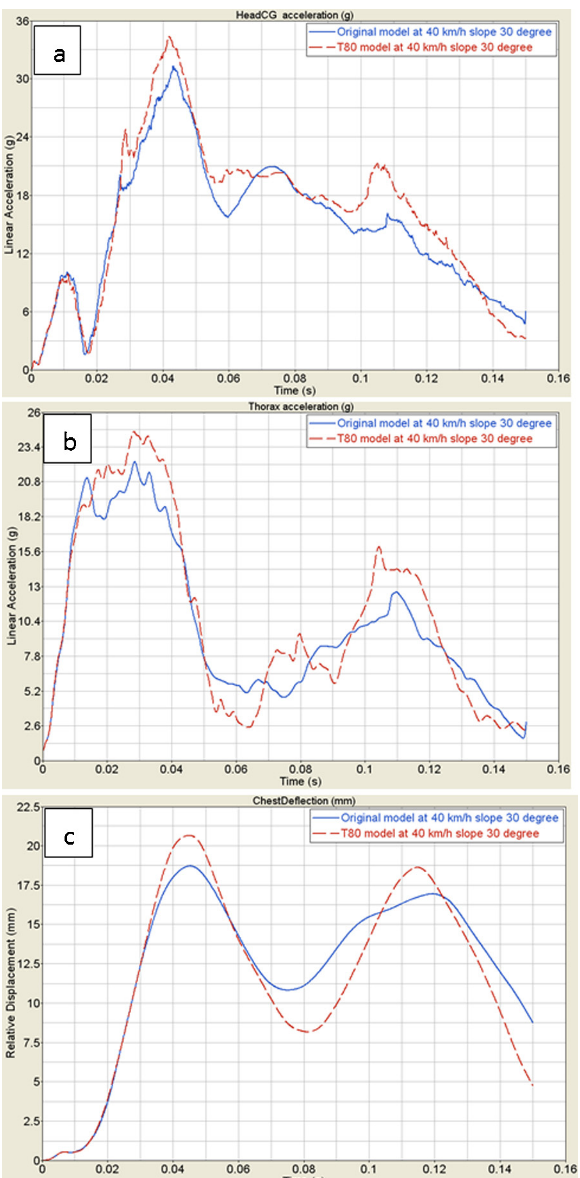

Fig. 9. Head acceleration (a), thorax acceleration (b), and chest deflection (c) for the original (solid line) and T80 (dash line) models at 40 km/h speed with 30 degree rotated barrier.

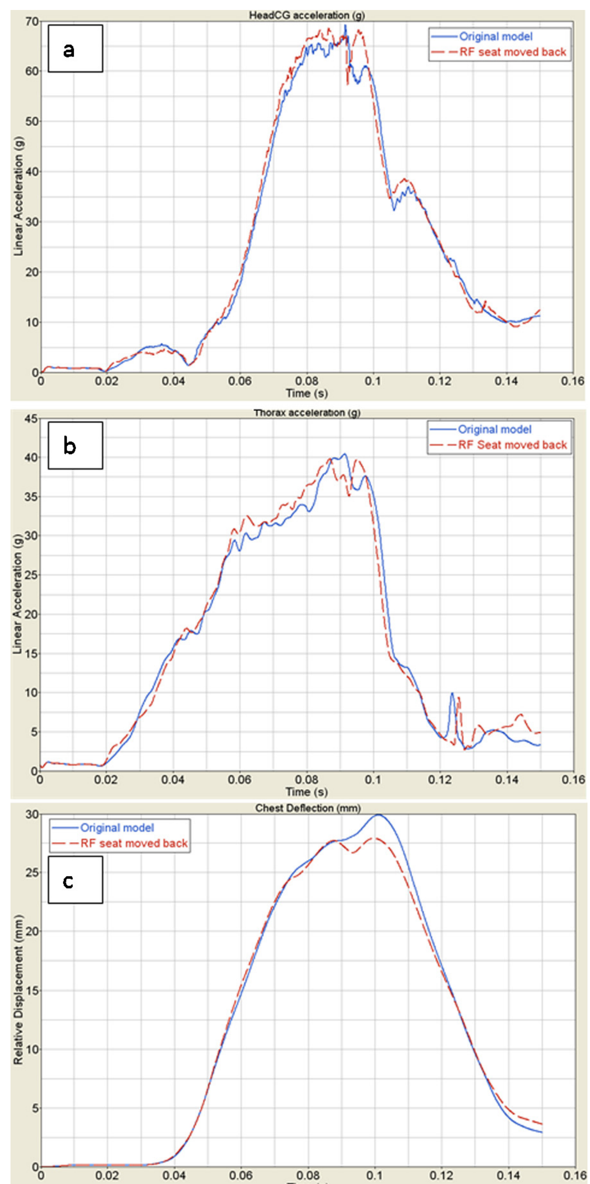

Fig. 10. Head acceleration (a), thorax acceleration (b), and chest deflection (c) for original model (solid line) versus the model with right front seat moved back (dash line).

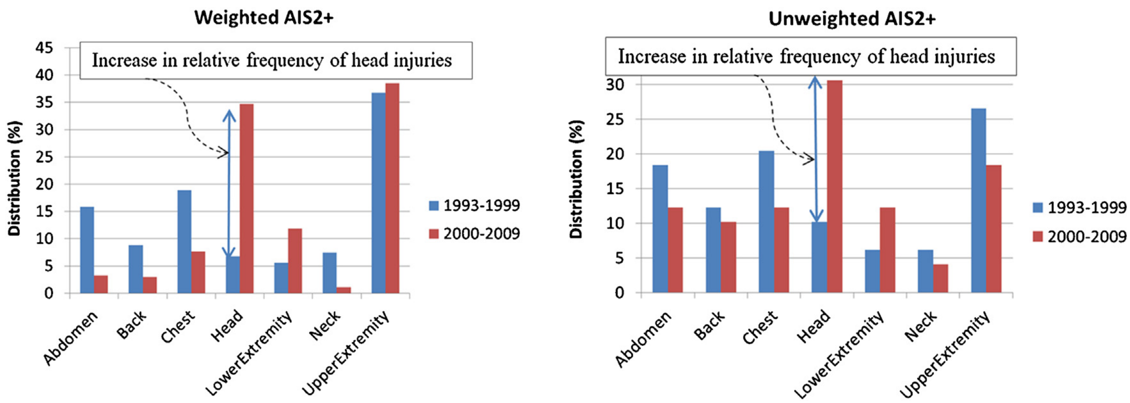

Fig. 11. Body region AIS2+ injury distribution for two model year groups of vehicle, occupants 16–59, weighted (left) and unweighted (right).

earlier contact of extremities with back of the front seat. Those contacts ultimately control the movement of the trunk, reduce the forward motion of the chest, and decrease the chest deflection. However, the overall difference between the injury measures for the original model and the reduced backseat space model seem trivial.

4. Discussions and limitations

This work was a concluding part of a series of studies done by the present authors (Sahraei et al., 2009, 2010, 2011; Sahraei and Digges, 2009). The studies were motivated to find the cause of the contradiction in a series of papers on the protection of the rear-seat occupant. One group of authors had concluded that the rear-seat occupants are better protected than the front seat occupants based on the analysis of real-world accident data (where the majority of the vehicles were built pre-2000) (Evans and Frick, 1988; Smith and Cummings, 2004, 2006). Whereas the other works showed the opposite, that the rear-seat occupant was less protected than the front (based on laboratory crash tests of post-2000 vehicles) (Kuppa et al., 2005; Tylko and Dalmotas, 2005). In initial investigations by present authors, the effect of the model year proved to be a significant factor. Meaning, in older model years, occupants were better protected in the rear seats, while the protection decreased in newer model years (Sahraei and Digges, 2009; Sahraei et al., 2009, 2010). In the next step, it was concluded that the most significant changing factors between the model years were the mass and front end stiffness, which increased with model years of vehicles (Sahraei et al., 2011).

Further studies of laboratory crash tests showed that an increase in mass was not negatively correlated with protection of the rear seat occupant, while an increase in stiffness was correlated with rear seat dummies HIC, 3-ms clip chest acceleration, and chest deflection (Sahraei et al., 2013). However, in crash tests there still could be other uninvestigated factors to influence the result. Therefore, a final piece of research, presented in the current paper, was devoted to finite element modeling, where one can keep all other possible contributing factors constant and only change stiffness. The vehicle stiffness can change due to using high strength steels or higher thickness of load bearing parts. The results showed an increase in stiffness, with either of those methods, increases the HIC, 3 ms chest acceleration, chest deflection, and N_{ij}. Furthermore, those injury criteria numbers were translated to AIS3+ risk of injury, and the results showed interesting observations regarding risk of head and chest injury. In the original model, the projected risk of AIS3+ chest injury for a 35-year-old occupant was 9.1% almost twice that of the risk of head injury (4.8%). While in the highest stiffness model (T80) the risk of AIS3+ head injury increased to 24.2%, almost twice as high of the risk of chest injury for a 35-year-old occupant (11.8%). This increase in risk of head injury was previously observed in investigations of real world accident data (Sahraei and Digges, 2009). To verify if further similarities could be observed in real world crashes, a study of the distribution of body regions injured in NASS CDS data, presented in an earlier publication by two of the present authors (Sahraei and Digges, 2009), was extended here. In the original study, all the model years of the vehicles were aggregated. For the present publication, the vehicles were divided to two model year groups, 1993–1999 and 2000–2010. Fig. 11 shows the weighted and unweighted distribution of AIS2+ injured body regions. What is interesting here is that in both graphs, after upper extremity injuries (which are usually not life threatening), chest injuries are the dominant injuries in 1993–1999 group of vehicles. However, in the 2000–2010 model year group, head injuries have an increase of two to three times and exceed the frequency of chest injuries in both weighted and unweighted data. Additionally, the proportion of head injuries in the 2000–2010 group is much larger than that of chest injuries. The age group of occupants in this data was 16–59 (average 37) year old. These results are fully aligned with findings of the FE simulations, which show a fivefold increase in risk of head injury from 4.8% to 24.2%, and a relatively slower rate of increase for the risk of chest injury from 9.1% to 11.8% for the 35 year old occupant. However, it should be mentioned that for the 60 year old occupant, the chest injury maintains the higher risk of over 30% even for the stiffest vehicle simulation. Risk of neck injury from simulations, if interpreted according to the NHTSA curve, would be more representative of the combined risk of neck and back (thoracolumbar spine) injuries. However, for the risk of neck injuries as a separate group, the risks estimated from Mertz et al. risk curve are more consistent with real world data.

Additionally, costs of AIS2+ injuries (HARM) for head and chest were calculated for pre and post 2000 model year vehicles. The average cost per injury values published by Gabler et al. (2005) was used to calculate the total costs. The costs were normalized to the cost of a fatality and to the number of occupants at risk. In the 1993–1999 model year group, the normalized cost of chest injuries was 0.15%, while that of head injuries was 0.07%. These values greatly change for the 2000–2010 model year vehicles to 0.17% and 0.42% for chest and head injuries, respectively. The HARM calculations again confirm the fast increase in head injuries in the newer model year group.

In the final parts of results, the simulations showed that these results were not limited to full frontal, 56 km/h impacts. The same trends were repeated when simulating low speed and oblique impacts.

Some of the limitations of this study are discussed below. (1) A generic seatbelt model was used rather than a validated model for the specific vehicle. This allows comparisons between models where changes in chest responses and torso kinematics can be attributed to the changes in stiffness and mass simulated, but limits direct comparison with real test data. (2) The simulations allowed a comparison of results when only mass or stiffness changes and other factors remain constant. The extent of effects of changes in stiffness and mass in real world vehicles could be less or more than what observed in simulations due to simultaneous improvements in safety systems or modifications in the body in white of the vehicles. For example, the effects of the increase in stiffness are completely overcome for front seat occupants by use of advanced airbags and load limiting pre-tensioning safety belts.

The purpose of the simulations presented in this paper was not to exactly replicate all the changes in model years of vehicles. Effects of overall changes in real vehicles are studied in previous publications using real world accident databases. Details of all changes that each manufacturer adopts through model years of vehicles are proprietary information of that company. The crash pulses in the simulations are not expected to perfectly match the NCAP tests, as slight changes in design, manufacturing methods, or materials may offset or intensify the simulated effects. What is evident from NCAP tests of all vehicles through two decades is that the stiffness of real vehicles has increased over time (Sahraei et al., 2013), and crash tests of vehicles with dummies in the rear seat show a correlation between injury measures and the front end stiffness when all the manufacturing changes are in place. This paper adds the following to the previous findings in literature: in the absence of any other change, an increase in stiffness would increase injury measures of dummies in the rear seat.

5. Conclusion

The increase in front–end stiffness of vehicles significantly increases the possibility of injury and particularly head injury for rear seat occupants. The increase in stiffness can be a result of using higher strength steels or thicker sheets of metal. The authors suggest that with the increase in stiffness of vehicles, the safety measures for protection of rear seat occupant should be updated. Otherwise, a significant increase in the number of younger rear seat adults with head injuries sustained from frontal crashes can be expected. For older rear seat occupants, chest injury would continue to be the most frequent injury and its risk would continue to increase in the stiffer vehicles. Possible remedies to reduce rear seat occupant injuries are use of airbags and advanced safety belts for rear seat passengers or improvements in crash energy absorption of vehicle structures.

Acknowledgments

Authors would like to thank Mr. Mark Shooter for his kind editorial assistance. Also, the support of Altair Company with providing the Hyper Work software to us is greatly appreciated.

Appendix A. Validation of finite element simulation against Crash Test 5143

Figs. A1–A4.

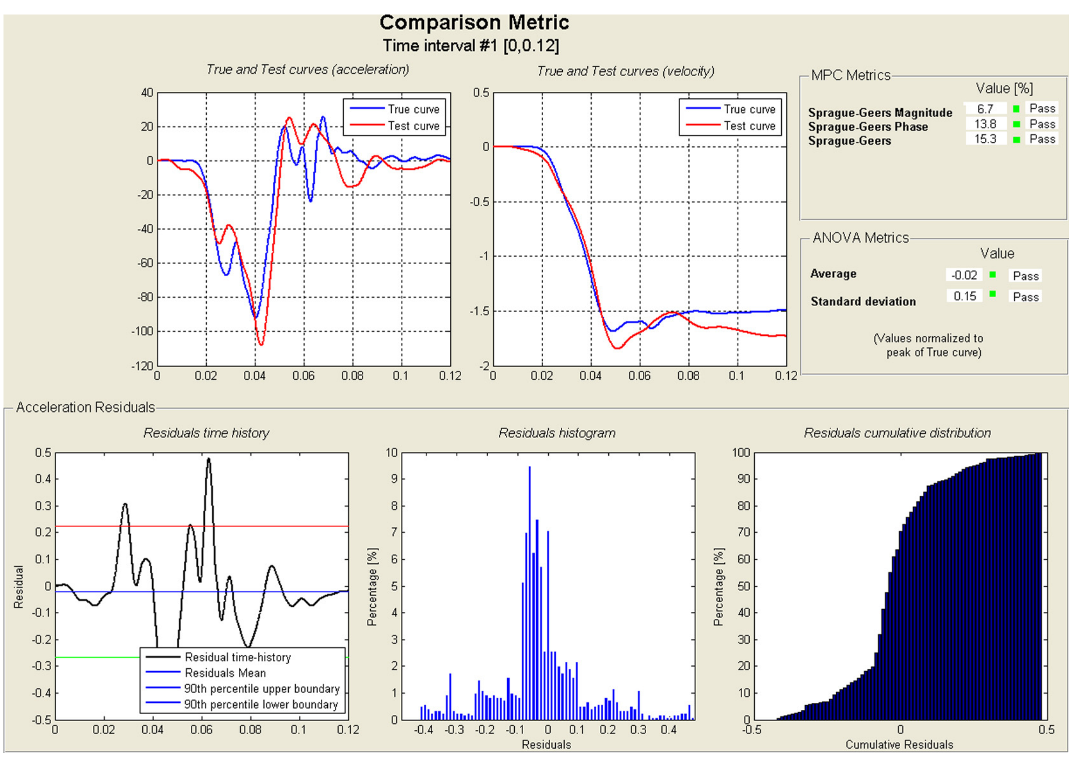

Fig. A1. Comparison metric for Engine X acceleration, Ford Taurus Vehicle, FE simulation versus test.

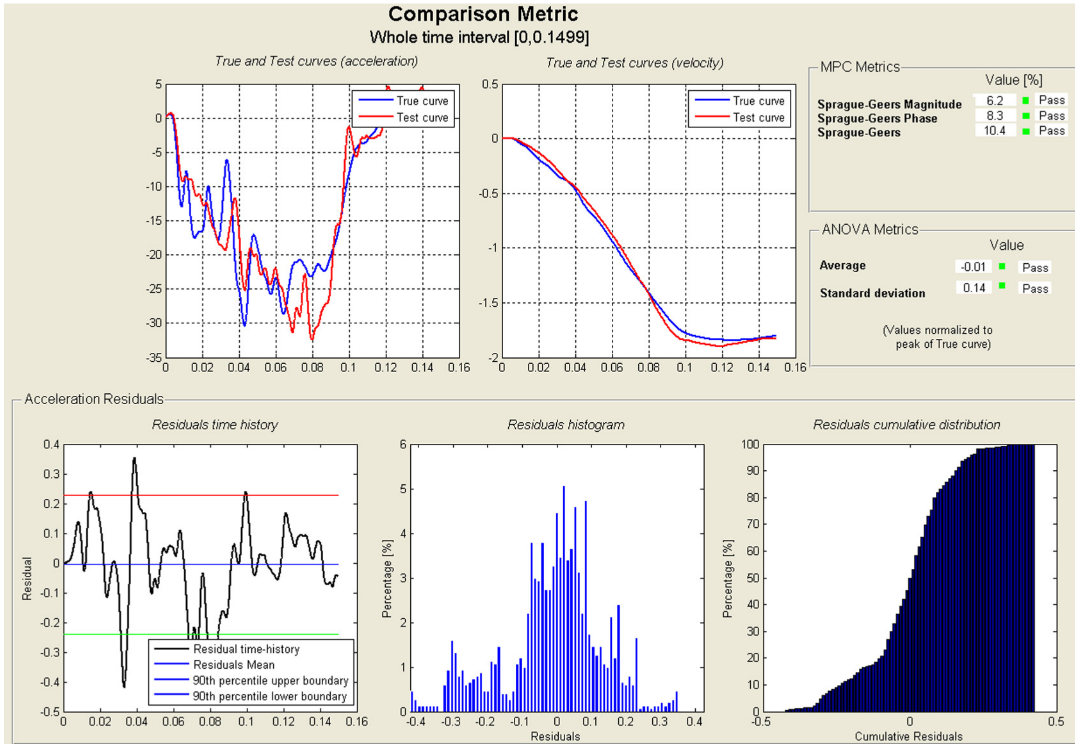

Fig. A2. Comparison metric for Left Rear Seat X acceleration, Ford Taurus Vehicle, FE simulation versus test.

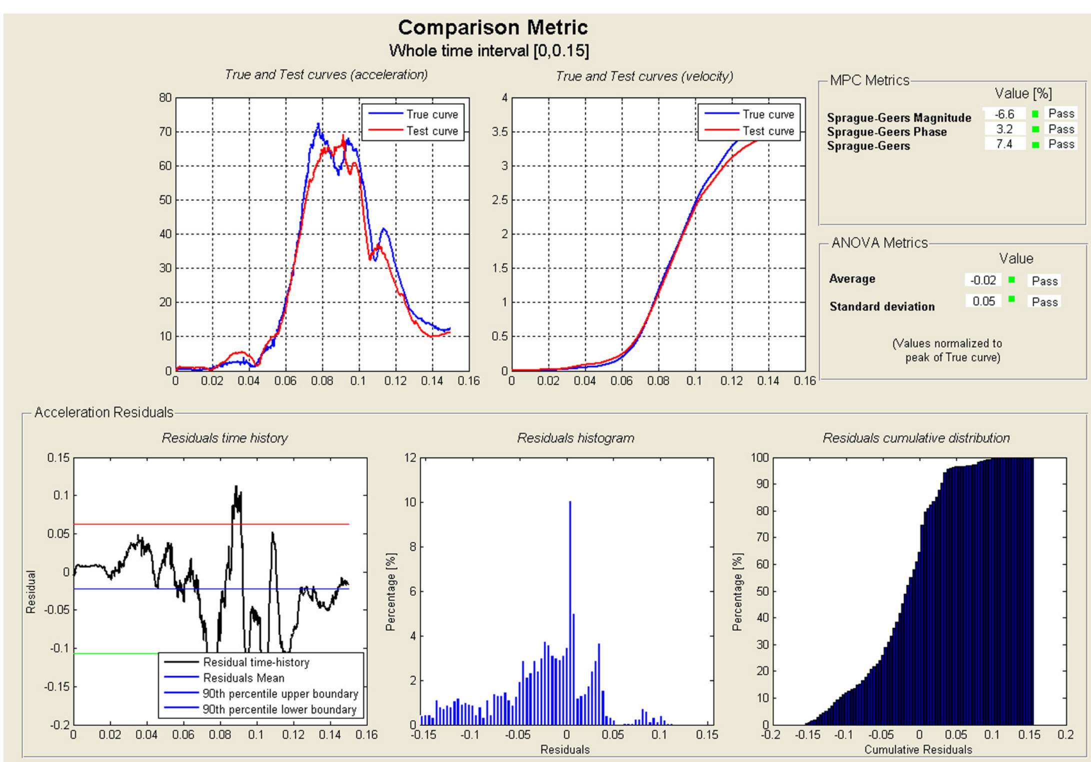

Fig. A3. Comparison metric for resultant head acceleration, 5% Female dummy, FE simulation versus test.

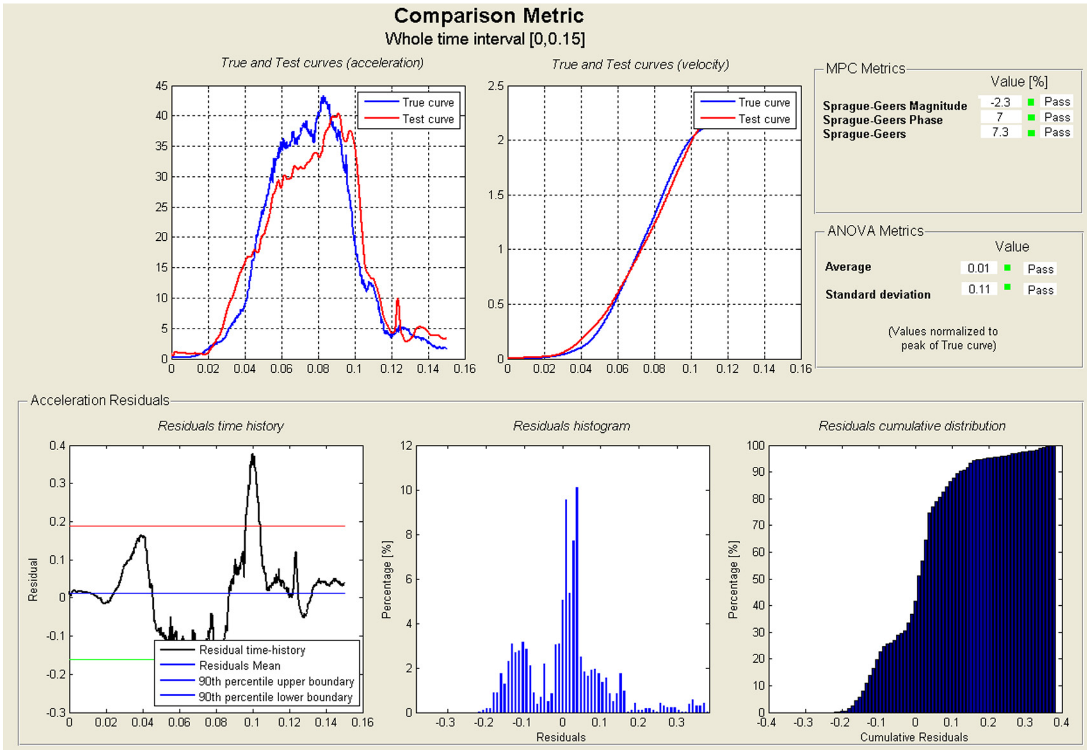

Fig. A4. Comparison metric for thorax acceleration, 5% female dummy, FE simulation versus test.

References

Beck B., Brown J., Bilston L., 2009. Development of occupant protection systems: leaving the rear seat behind. In: 2009 Australian Road Safety Research, Policing and Education Conference, Sydney, NSW, pp. 787–795.

Berg, M., Cook, L., Corneli, H., Vernon, D., Dean, J., 2000. Effect of seating position and restraint use on injuries to children in motor vehicle crashes. Pediatrics 105 (4), 831–835.

Bilston, L.E., Du, W., Brown, J., 2010. A matched-cohort analysis of belted front and rear seat occupants in newer and older model vehicles shows that gains in front occupant safety have outpaced gains for rear seat occupants. Accid. Anal. Prev. 42 (6), 1974–1977.

Eppinger, R., Sun, E., Kuppa, S., Saul, R., 2000. Supplement: development of improved injury criteria for the assessment of Advanced Automotive Restraint Systems—II. In: Docket No. 7013. NHTSA.

Evans, L., Frick, M., 1988. Seating position in cars and fatality risk. Am. J. Public Health 78 (11), 1456–1458.

Gabler, H.C., Fitzharris, M., Scully, J., Fildes, B.N., Digges, K., Sparke, L., 2005. Far side impact injury risk for belted occupants in Australia and the United States. In: Proceedings of the 19th International Conference on Enhanced Safety of Vehicles, Washington, DC.

Hertz, E., 1993. A note on the head injury criterion (HIC) as a predictor of the risk of skull fracture. Proc. Assoc. Adv. Automot. Med. Annu. Conf. 37, 303–312.

Kent, R., Forman, J., Parent, D., Kuppa, S., 2007. The feasibility and effectiveness of belt pretensioning and load limiting for adults in the rear seat. Int. J. Veh. Saf. 2 (4), 378–403.

Kuppa, S., Saunders, J., Fessahaie, O., 2005. Rear seat occupant protection in frontal crashes. In: 19th International Conference on Enhanced Safety of Vehicles, Washington, DC.

Laituri, T.R., Prasad, P., Sullivan, K., Frankstein, M., Thomas, R.S., 2005. Derivation and evaluation of a provisional, age-dependent, AIS3+ thoracic risk curve for belted adults in frontal impacts. In: SAE World Congress, Detroit, MI.

Laituri T., Kachnowski B., Prasad P., Sullivan K., Przybylo P., 2003. A theoretical, risk assessment procedure for in-position rivers involved in full-engagement frontal impacts. In: SAE World Congress, Detroit, MI.

Mertz, H., Irwin, A., Prasad, P., 2003. Biomechanical and scaling bases for frontal and side impact injury assessment reference values. Stapp Car Crash J. 47, 155.

Mertz, H., Prasad, P., Irwin, A., 1997. Injury risk curves for children and adults in frontal and rear collisions. In: SAE World Congress, Detroit, MI, pp. 13–30.

Mertz, H., Prasad, P., Nusholtz, G., 1996. Head injury risk assessment for forehead impacts. SAE Trans. 105 (6), 26–46.

Mongiardini, M., Ray, M., 2009. Roadside Safety Verification and Validation Program (RSVVP), Rev. 1.3.

NCAC, 2008. National Crash Analysis Center Vehicle Model Library. NCAC, http://www.ncac.gwu.edu/vml/models.html.

NHTSA, 2008. Federal register consumer information; New Car Assessment Program. In: Docket No. NHTSA-2006-26555. NHTSA, 73, Notice, No. 134.

Oliver, S., Jones, T., Fourlaris, G., 2007. Dual phase versus TRIP strip steels: comparison of dynamic properties for automotive crash performance. Mater. Sci. Technol. 23 (4), 423–431.

Parenteau, C., Viano, D., 2003. Field data analysis of rear occupant injuries—Part I: Adults and teenagers. In: SAE World Congress, Detroit, MI.

Prasad, P., Mertz, H., 1985. The position of the United States Delegation to the ISO Working Group 6 on the use of HIC in the automotive environment (851246). In: SAE Government Industry Meeting, Warrendale, PA.

Prasad, P., Mertz, H., Dalmotas, D., Augenstein, J., Digges, K., 2010. Evaluation of the Field Relevance of Several Injury Risk Functions. Stapp Car Crash J. 54, 49–72.

Ray, M., 1996. Repeatability of full-scale crash tests and criteria for validating simulation results. Transp. Res. Rec.: J. Transp. Res. Rec. 1528 (1), 155–160.

Sahraei, E., Digges, K., Marzougui, D., 2013. Effects of vehicle front-end stiffness on rear seat dummies in NCAP and FMVSS208 Tests. Traffic Inj. Prev. 14 (6), 602–606.

Sahraei, E., Marzougui, D., Digges, K., Kan, C., 2011. Effect of increase in weight and stiffness of vehicles on the safety of rear seat occupants. Int. J. Crashworthiness 16 (3), 309–318.

Sahraei, E., Digges, K., 2009. Trend of rear occupant protection in frontal crashes over model years of vehicles. In: SAE World Congress, Detroit, MI.

Sahraei, E., Digges, K., Marzougui, D., 2010. Reduced protection for belted occupants in rear seats relative to front seats of new model year vehicles. Ann. Adv. Automot. Med. 54, 149–158.

Sahraei, E., Soudbakhsh, D., Digges, K., 2009. Protection of rear seat occupants in frontal crashes, controlling for occupant and crash characteristics. Stapp Car Crash J. 53, 75–91.

Smith, K., Cummings, P., 2006. Passenger seating position and the risk of passenger death in traffic crashes: a matched cohort study. Inj. Prev. 12 (2), 83–86.

Smith, K., Cummings, P., 2004. Passenger seating position and the risk of passenger death or injury in traffic crashes. Accid. Anal. Prev. 36 (2), 257–260.

Swanson J., Rockwell T., Beuse N., Summers L., Summers S., Park B., 2003. Evaluation of stiffness measures from the U.S. new car assessment program. In: 18th International Conference on Enhanced Safety of Vehicles, Nagoya, Japan, pp. 03–0527.

Tylko S., Dalmotas D., 2005. Protection of rear seat occupants in frontal crashes. In: 19th International Conference on Enhanced Safety of Vehicles, Washington, DC, pp. 05–258.